Use of 1km²-resolution imagery in the Belgian Crop Growth Monitoring System (B-CGMS)♦

Herman Eerens♠, Katty Wouters♠, Dominique Buffet♥, Robert Oger♥, Didier Dehem♣, Bernard Tychon♣

♠ *Centre of Expertise on Remote Sensing and Atmospheric Processes (Vito-TAP)*
Boeretang 200, B-2400 Mol, Belgium *E-mail: herman.eerens@vito.be*
♥ *Centre de Recherches Agronomiques (CRA)*
Rue de Liroux 9, B-5030 Gembloux, Belgium *E-mail: oger@cragx.fgov.be*
♣ *Fondation Universitaire Luxembourgoise (FUL)*
Avenue de Longwy 185, B-6700 Arlon, Belgium *E-mail: tychon@ful.ac.be*

Abstract

The Belgian Crop Growth Monitoring System (B-CGMS) uses the 1km²-resolution imagery of NOAA-AVHRR and SPOT-VEGETATION to improve its yield estimates. The pre-processed images are converted to fAPAR and combined with meteorological data (irradiance, temperature) to daily growth values by means of the Monteith approach. The regional means of the cumulative monthly growth numbers are calibrated against official harvest statistics by means of crop-specific neural networks. The quality of the yield estimates varies with the importance of the crop: the R²-values for winter wheat, sugar-beets and fodder maize are respectively 60%, 48% and 36%. The final yield forecasts will be better, because the B-CGMS integrates the image-based yield estimates with the assessments of the agromet-model and of the technological trend function. The technique of linear unmixing seems promising but in its actual state it is too unpredictable to be included in an operational scheme.

1. Context and Objectives

One of the major achievements of the European MARS-programme (Monitoring Agriculture with Remote Sensing) was the Crop Growth Monitoring System. Since a few years, this CGMS is used on a continuous base to predict harvests and productions of the main crops in the EU member states (Vossen & Rijks, 1995). Actually, the crop yield estimates of the CGMS are the integrated result of three independent procedures: a spatialized agrometeorological model, a trend function which copes with the long-term increases due to technological improvements, and the information provided by the 1km²-resolution imagery of the remote sensing system NOAA-AVHRR.
In 1998, a project was started in order to implement a specific version of the CGMS in Belgium. This so-called B-CGMS will allow the Belgian Ministry of Agriculture to generate its own predictions in a timely way. To this goal, the original EU-CGMS was improved or adapted in the following ways:

- The spatial scale of the system was enhanced, such that the agrometeorological model now runs on 10x10km² cells (instead of 50x50km² before).
- More detailed pedological and meteorological information was collected and introduced into the model. Crop parameters were also chosen typically for the Belgian conditions.
- The crop surfaces, needed to assess the productions, are derived from the Integrated Administration and Control System (IACS) of the Ministry of Agriculture. This yearly updated, vectorial GIS comprises the boundaries and crop type for all agricultural parcels (± 600 000).
- Whereas the original CGMS only deals with NUTS-level 1 (territory, Flanders, Wallonia), the B-CGMS provides specific forecasts for each of the 14 agricultural regions and/or each of the 26 agro-statistical circumscriptions.

Currently, the adapted system is validated on a 15-years series of yield data, obtained from the National Institute for Statistics (NIS). This paper however deals with the remote sensing part of the project. In addition to the above-mentioned targets, special efforts were made to obtain a better integration of the satellite imagery in the yield forecasting system. Besides the classical NOAA-AVHRR, use was also made of the 1km²-imagery of the recently launched earth observation system SPOT-VEGETATION (VGT).

♦ The B-CGMS project can be consulted at: http://b-cgms.cragx.fgov.be.

2. General Approach

As a basic approach for the inference of yield estimates from remote sensing images, daily increases ΔW in dry matter (DM) biomass were computed by means of the widely applied equation of Monteith (1972):

$$\Delta W = S_{par} \bullet fAPAR \bullet \varepsilon(T) \qquad [kgDM/ha/day]$$

S_{par} is the incoming Photosynthetic Active Radiation in J/ha/day (± 50% of the short-wave spectrum of the sun), *f*APAR is the fraction absorbed by the living vegetation, and ε(T) is the conversion efficiency in kgDM/J which is simply modelled here as a function of the daily mean temperature T (see Sabbe et al., 1999). The necessary meteorological data (S_{par} and T) and the *f*APAR-values were respectively extracted from the B-CGMS databases and the satellite images. The obtained daily growth numbers can be summarized in two ways: in a temporal sense cumulative values W [kgDM/ha] can be computed for specific periods, while in a spatial sense regional averages can be derived.

A parcel-based application of the Monteith approach is a priori excluded, due to the low resolution of the imagery and the small mean parcel size. The large majority of the 1km²-pixels are "mixed pixels", which are covered by different parcels and land use classes, and hence yield a mixed optical signal. Two alternative methods were evaluated to overcome this problem and to obtain crop-specific yield estimates. First, the classical procedure for linear unmixing was tried out in order to retrieve pure crop signals (see §4). But so far this technique could not be brought to an operational stage. The second method thus simply accepts the mixed nature of the satellite signals and tries to infer crop-specific yield estimates by calibration of image-derived indicators against official harvest data (see §5).

3. 1km²-Resolution Imagery: Data Sets and Preparation

Table 1 gives an overview of the 6 available, yearly image sets: 4 from AVHRR and 2 from VGT. Inspection of the data sets pointed out the superior quality properties of VGT. The SPACE-II AVHRR-data were badly registered (see figure 1.B) and contained a lot of anomalies (missing values/images, striping effects, etc). All syntheses suffered from a very important cloud noise.

***Table 1**: Overview of the used image sets*

Feature	NOAA-AVHRR	SPOT-VEGETATION (VGT)
Period	4 years: Jan. 1995 - Dec. 1998	2 years: April 1998 – Dec. 1999
Imagery Type	S1: 365/6 daily syntheses / year	S10: 36 decadal syntheses / year
Pre-Processing	SPACE-II (JRC)	CTIV (CNES, Vito)
Projection & Resolution	Albers Equal Area (1.1 km)	Geographic Lon/Lat (1°/112)

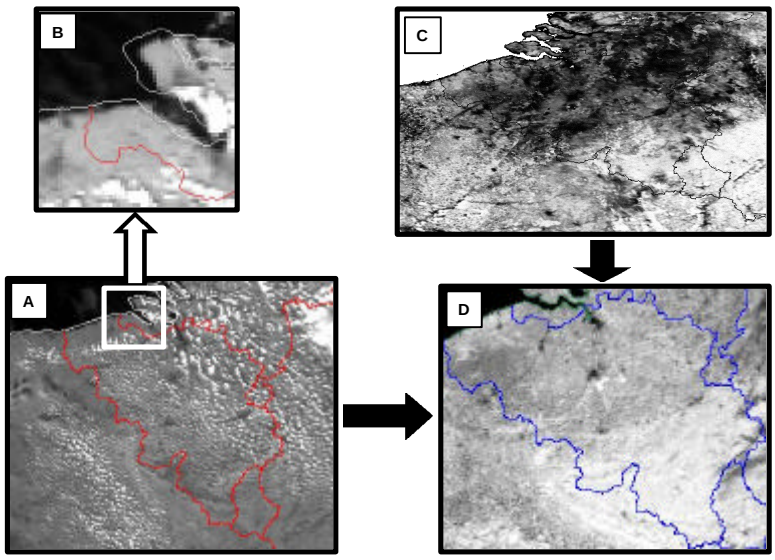

***Figure 1**: Cartographic conversions*

A. Albers Conic Equal Area (AVHRR, S1, NIR-band)

B. Idem, but zoom-in over Zeeland

C. Unprojected Lon/Lat-system (VGT, S10-synthesis, NDVI)

D. Belgian Lambert Conic Conform (B-CGMS reference, NDVI)

For this research, only the NDVI-information was used (Normalized Difference Vegetation Index). The six available, full-year image sets were processed as follows:

- The NDVI image layers were unpacked from their specific formats and compiled into one single image file per year (365/6 layers for AVHRR, 36 layers for VGT).
- The data were reprojected towards the B-CGMS system (see figure 1.D).
- The NDVI-profiles were cleaned to eliminate the cloud noise (see figure 2).
- The NDVI-data were then converted into *f*APAR-images by means of sensor-specific linear equations (*f*APAR = A + B.NDVI) whose parameters were obtained by means of a simple histogram-analysis (AVHRR: A = –0.27, B = 1.68; VGT: A = –0.25, B = 1.54).

In a technical sense (i.e. omitting the intrinsic quality properties), after these preliminary operations both data types (AVHRR, VGT) were completely homogenized.

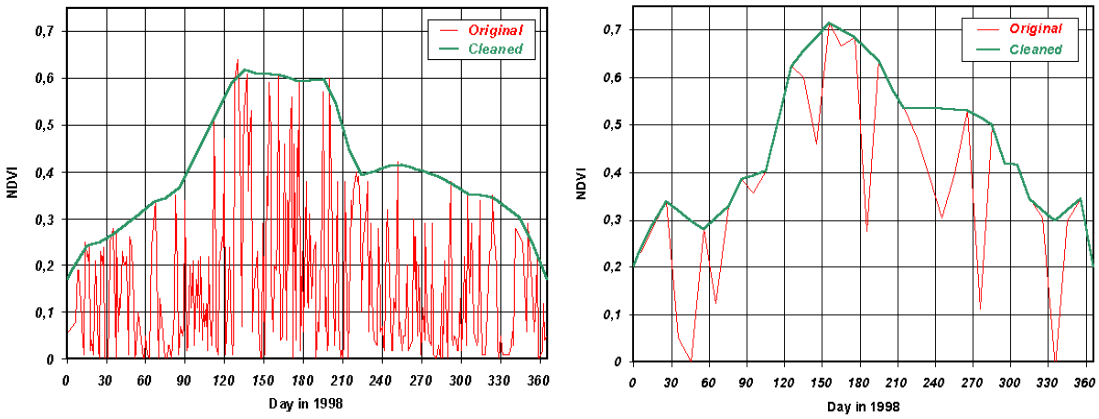

***Figure 2**: Evolution of the NDVI in 1998 for 2 pixels: original series extracted from the daily syntheses of NOAA-AVHRR (left) and from the decadal syntheses of SPOT-VGT (right). The abrupt local minima are mostly due to clouds. The "envelope" curves (thick lines) are the result of the cleaning procedure.*

4. Linear Unmixing

The method of linear unmixing assumes that the optical signal y_p, registered for the mixed 1km²-pixel p, is equal to the weighted average of the pure signals x_k of the N_k individual terrain classes/crops, with the sub-pixel surface fractions f_{pk} as weights ($y_p = \Sigma f_{pk}.x_k$). For a homogeneous area of N_p pixels one obtains a system of N_p equations, from which the pure signals x_k (regional means) can be retrieved with a simple matrix inversion. In this case, the required surface fractions f_{pk} could be extracted from the IACS-data set of the Ministry of Agriculture (see §1). All the non-agricultural destinations, not mentioned in the IACS, were assigned to a single "garbage" class (mostly built-up areas and forests).

The technique was first tried out with three high-resolution images of SPOT-XS, with a pixel size of 20x20m². The images were of 3 different dates in 1997 and they all covered an area of 800 km² in the Hesbaye region, ± northwest of the city of Liège. By confronting these high-resolution data with the IACS-information (vectorial parcel map with crop type for each field), the true x_k-values could be computed in advance. On the other hand, by degradation of the 20x20m²-imagery (taking the mean signal of each cell of 50x50 high-resolution pixels), equivalent low-resolution scenes were simulated with N_p = 800 1km²-pixels. The procedure for linear unmixing was then applied to the latter degraded scenes, and the resulting x_k-estimates were compared with the correct values. These validation tests pointed out that the relative errors (100.(true-estimated)/true%) were generally quite limited and mostly below 10%. This observation agreed fairly well with the findings of Cherchali et al. (2000) who performed a quite similar analysis.

The technique worked equally well for the three registration dates (1997: May 30, August 6, September 17) and for the different "optical signals": the individual red and near infrared reflectances and the NDVI. Several classification legends were tried out (from 15 classes to 0/1-systems like wheat vs. non-wheat) as well as various pixel selection methods (e.g. only use the 1km²-pixels which are covered for more than 50% by main crops), but none of these modalities appeared to have a clear and unambiguous influence on the performance of the unmixing technique.

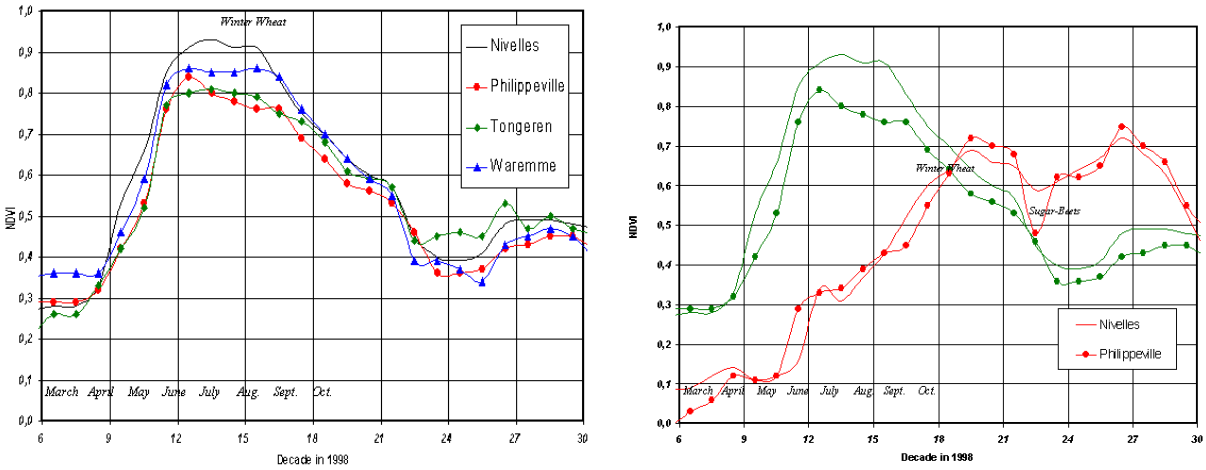

***Figure 3**: Pure NDVI-profiles in 1998 for winter wheat and sugar-beets in different agro-statistical circumscriptions, derived by linear unmixing from the (previously cleaned) image set of SPOT-VEGETATION.*

After this validation, the linear unmixing was applied to the real 1km²-imagery of AVHRR and VGT (cleaned NDVI-data). The method was repeated for each of the 26 agro-statistical circumscriptions (Np ≈ 1200) and for each image date, which resulted in temporal NDVI-profiles such as shown in figure 3. These examples reflect fairly well the common agricultural practices in Belgium. Winter wheat restarts its growth by the end of March, it culminates around May, ripens in June-July and is finally harvested in August. The later evolutions are of course irrelevant and vary per parcel. The same holds for sugar-beets in early spring. This crop starts its typically slow growth around May, with the leaf area culminating between July and September.

The unmixed, pure class profiles (x_k) show significantly higher dynamics than the mixed 1km²-signals (y_p). As far as only terrestrial pixels are concerned, the latter are mostly restricted to the NDVI-range 0.15 ... 0.75, while the unmixed NDVI's rather vary between 0.1 and 0.95. Obviously, the quality of the results will also depend on the spatial agreement between imagery and land cover data (IACS). It thus might not surprise that the best results were obtained for the images of SPOT-VGT. The poorer performance for NOAA-AVHRR is certainly due to the less accurate geometric correction.

The unmixed NDVI-profiles can in principle be used in the Monteith approach (after conversion to *f*APAR-values) to obtain crop-specific growth values on a regional base. However, the results were not always as good as in the examples of figure 3. In practice, the method appeared quite unpredictable and in many cases it yielded nonsensical NDVI-curves. Further research is certainly recommended, but for the time being the linear unmixing is not operational and as a consequence it had to be rejected in favour of the procedure described hereafter.

5. Image-Based Yield Indicators calibrated with Neural Networks

The different versions of this approach always start with the Monteith-computation of the daily growth values ΔW [kgDM/ha/day] on a per-pixel base (i.e. without differentiation between crops). The results are then accumulated over specific periods to DM-biomasses W [kgDM/ha]. Next, regional averages are derived for each of the 26 agro-statistical circumscriptions. This aggregation step only takes into account the pixels which are covered for more than 50% by cropland (criterion checked with the IACS

data set). Finally, crop-specific yield estimates (y_{est}) are defined by calibration of this set of yield indicators (1 or more x_i) against the official harvest statistics (y_{true}). The numbers of available data points per crop are mentioned in table 2 (at most: 6 yearly image sets x 26 circumscriptions = 156).

Our first trial was based on the dry matter biomass W accumulated over the entire growing season of each crop (see table 2 for the specific seasons). In spite of its logic and simplicity (1 single x-indicator), this attempt completely failed. The obtained R^2-values balanced around zero, probably because the approach gives equal weights to every moment in the season, while in practice each crop has its specific critical moments (e.g. flowering for the cereals).

With this lesson in mind, a more refined and multivariate procedure was elaborated which was calibrated separately for each crop with a three-layer "neural network with backpropagation training", as described by Paola & Schowengerdt (1995). The input layer of this network comprises 4-6 nodes, which are fed with the biomasses W accumulated for each month in the crop's growing season (4-6 x_i-values, see "Inputs" in table 2). The hidden layer counts three nodes and the output layer only one: the final crop yield. These networks were calibrated with the official statistics of the NIS (y_{true}). The number of parameters (neural weights) to be estimated in the calibration amounts to about 21. With ±150 data points per crop, this is perfectly feasible. However, in order to achieve an independent and reliable validation, the "Jackknife" method was applied. The sequence 'calibration-validation' was repeated in different steps, and in every iteration 10 data points were selected at random. The network was then trained with the remaining ±140 observations and validated with the 10 test points. This scheme was repeated until each point was used once for validation.

***Table 2**: Results of the image-based procedure for yield assessment (neural network + independent "Jackknife" validation): N=number of data per crop, RMSE=Root Mean Square Error (ton/ha), Y_{min}/Y_{max}=extreme values (ton/ha) in the NIS-data set (1995-1999, 26 circumscriptions).*

CROP	N	INPUTS	R %	R^2 %	RMSE	Y_{min}	Y_{max}
Winter wheat	155	6 (March-August)	77.3	59.8	0.8	2.9	10.8
Sugar-beets	138	6 (May-October)	69.5	48.4	5.3	34.8	80.0
Fodder maize	155	6 (April-September)	59.8	35.8	3.7	28.4	58.6
Winter barley	144	5 (March-July)	46.4	21.5	0.9	3.0	9.3
Potatoes	149	5 (April-August)	36.3	13.2	8.2	7.6	57.4
Winter rapeseed	81	4 (March-June)	26.1	6.8	0.5	2.0	4.5

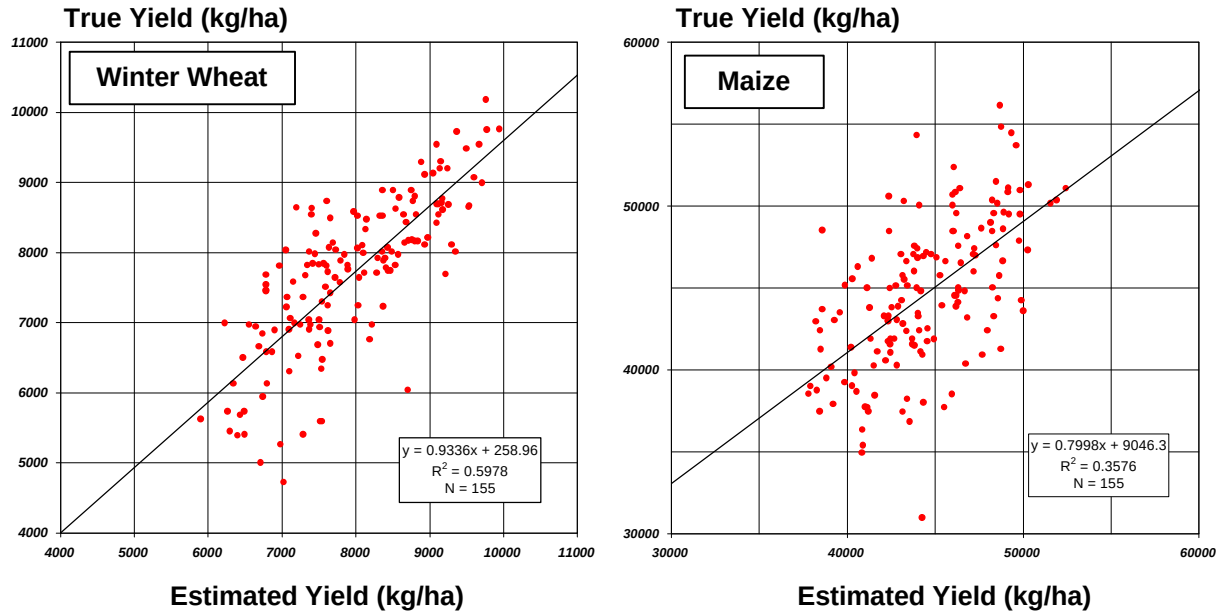

***Figure 4**: Official yields of the National Institute for Statistics (NIS) vs. the image-based estimations (neural networks) for winter wheat and fodder maize (see table 2).*

The validation results, presented in table 2, prove that the images of AVHRR and VGT do contain relevant information on the yield of the main crops, in spite of their low resolution. The R^2-values, which represent the fraction of the total variance explained by the image-based estimates, vary in function of the relative importance of the crops. The procedure works very well for winter wheat (R^2=59.8%) and somewhat less for sugar-beets (R^2=48.4%) and fodder maize (R^2=35.8%). The performance clearly decreases for the minor crops, especially for rapeseed (R^2=6.8%).

6. Conclusions

The validation results of table 2 only relate to the accuracy of the image-based procedure. The final yield assessments of the B-CGMS will probably be more reliable, because they are not only based on the remote sensing imagery but also on the outputs of the agromet-model and the technological trend function.

The described procedure only dealt with the problem of "yield estimation" where one disposes of all the information (images, meteo) until the end of the on-going year. Nevertheless, the neural network methodology is flexible and it can be used as well for the more difficult task of "yield forecasting". For each situation, a specific calibration must be executed in advance. In this way, the method could for instance be applied at the end of May to predict the final yields of wheat and barley.

This work also demonstrated that the combined use of SPOT-VEGETATION and NOAA-AVHRR does not raise any problem. Linear unmixing of the compound signal of the 1km²-pixels can best be applied on the VEGETATION-images because of their high geometric precision. This important topic however requires further investigation, before it can be integrated in an operational yield forecasting scheme.

Acknowledgements

This project was financed by the Belgian Ministry of Agriculture, the Federal Office for Scientific, Technical and Cultural Affairs (OSTC), and the Flemish Institute for Technological Research (Vito). The meteorological data, official yield statistics and part of the images (NOAA-AVHRR, SPOT-XS) were respectively provided by the Royal Meteorological Institute, the National Institute for Statistics and the EU-Joint Research Centre (Italy).

References

Cherchali S., Amram O. & Flouzat G., 2000, *Retrieval of temporal profiles of reflectances from simulated and real NOAA-AVHRR data over heterogeneous landscapes*, Int. J. Remote Sensing, 21: 753-775.

Monteith J.L., 1972, *Solar radiation and productivity in tropical ecosystems*, J. Applied Ecology, 19: 747-766.

Paola J.D. & Schowengerdt R.A., 1995, *A review and analysis of backpropagation neural networks for classification of remotely-sensed multi-spectral imagery*, Review article, Int. J. Remote Sensing, 16: 3033-3058.

Sabbe H., Eerens H. & Veroustraete F., 1999, *Estimation of the carbon balance of European terrestrial ecosystems by means of the C-Fix model*, Proc. "1999 EUMETSAT Meteorological Satellite Data Users' Conference", 6-10 Sept. 1999, Copenhagen, Denmark, 271-278.

Vossen P. & Rijks D., 1995, *Early crop yield assessment of the EU countries: the system implemented by the Joint Research Centre*, EUR Publication 16318 EN, 1995, JRC, Italy.